European Journal of Scientific Research
ISSN 1450-216X Vol.24 No.2 (2008), pp.197-210

http://www.eurojournals.com/ejsr.htm

Theoretical and Computational Modelling of Pseudo-Damage Induced Approach for Failure Prediction of Low Velocity Impact on Fibrous Composite Panels

Umar Farooq
Built Environment and Engineering Department
University of Bolton, BL3 5AB, United Kingdom
E-mail: uf1res@bolton.ac.uk

Karl Gregory
Built Environment and Engineering Department
University of Bolton, BL3 5AB, United Kingdom
E-mail: k.r.gregory@bolton.ac.uk

Abstract

Computational model of pseudo-damage induced stiffness parameters and static load-deflection response was developed to study the initiation and propagation of barely visible impact damage (BVID) and failure prediction of composite panels.

The mathematical model consisting of constitutive, equilibrium, and strain-displacement relations for the impact damage phenomena was developed. The damage dependent failure criteria proposed by Tsai-Hill and Tsai-Wu were used to predict ply failures.

Computer code for the model was implemented using the commercially available software package 'ABAQUS'. Simulations were carried out inducing progressive-damage in the local area of a ply under load considering damage modes of matrix cracks, fibre-breakage, fibre/matrix de-bonds, and de-laminations leading to eventual failure. To improve convergence adaptive meshing techniques were employed to mesh the high stress gradient areas with fine meshes and coarse meshes for the rest. Simulations were performed for un-damaged and damage induced responses of various specimens of different ply orientations until first ply failure occurs.

The approach involves simple steps in which simulations are repeated after pseudo damage is induced to predict stresses for properties of degraded sub-laminate plies. Simulation for load-deflection was also carried out for virgin and pseudo-damaged models.

The study indicates that the approach is useful, easier and economical to model. The output results and data could be used for predicting the performances of composite structures to develop reliable and safe designs that exploit the advantages offered by composites.

Keywords: Composite structures, low-velocity impact, de-lamination, finite element simulation

1. Introduction

There is an increasing demand in the aerospace industries for high-performance composite structures with high strength, high modulus, low weight, and good damage resistance properties. However, composite structures are susceptible to out-of-plane impact loading that remains a great challenge to model due to its geometric and material nonlinearities. It is also difficult to study applying conventional theories, and numerical methods. Therefore, there is no standard method to predict comprehensive failure criteria.

While designing a composite system it is not feasible to test all vulnerable surfaces of a structure for reliable and safe design parameters, hence a computational model is needed. Some of the following important studies related to the impact damage on composite panels in the literature are presented as follows.

Matrix properties governing the damage initiation and fibre properties controlling the penetration resistance were studied experimentally by Elber in (Elber, 1985). Dynamic loading and characterization of fibre-reinforced composites were studied by Sierakowski in (Sierakowski, 1997). Stress analysis of orthotropic laminated slabs to transverse load was studied by Matsumoto in (Matsumoto, 1992).

A new approach to damage mechanisms and mechanics of composites due to low-velocity impact' was performed by Choi, H.Y., Downs, R. J., and Chang, F. K., in (Choi, 1991). A predicting model for graphite/epoxy composites low-velocity impact based on experimental observations was presented by Choi, H.Y. and Chang, F. K., see (Choi, 1992). A quasi-static treatment of de-lamination crack in laminates subjected to low velocity impact was presented by Sun, C. T. and Jih, C. J., in the Proceedings of 7th Technical Conference see (Sun, 1995). Experimental investigation on Penetration of kevlar by projectiles- I., was studied by Zhu, G., Goldsmith, W., and Dharan, C. K. H., (Zhu, 1992).

On the Fracture Mechanics side, it was shown that the strain energy release rate computed from static and dynamic analysis was in good agreement with experiment on Penetration of glass/epoxy composite laminates was studied by Wu, E., Tsai, C. Z. and Chen, Y. C., (Wu, 1994). Impact on laminated composites was published by Abrate, S., in recent advances, Applied Mechanics Reviews (Abrate, 1994). Quasi-static ballistic perforation of carbon fibre laminates was studied by Goldsmith, W., Dharan, C. K. H., and Chang, H., (Goldsmith, 1995).A model to predict residual velocity of thick composite to high velocity impact by Sun, C. T. and Potti, S. V., see (Sun,1996). A quasi-static penetration model for composite laminates was studied by Lee, S. W. R. and Sun, C. T. in (Lee, 1993). Investigation of successive failure modes in graphite epoxy comp panels by Greif, R. and Chapon, E. see (Greif, 1993). Survey of integral formulation for non-local damage analysis models were carried out in Progressive failure analysis of composite panels by Kim, Y., Davalos, J. F. and Barbero, E. J., in (Kim, 1996). Luo derived a three-dimensional model analytical solution of clamped circular plates by taking displacement as the basic variable; however, their analysis involves a step to solve ordinary differential equations, and hence is very cumbersome see (Luo et al., 2004).

Impact Damage Resistance and Damage Tolerance of Fibre Reinforced Laminate Composites were investigated by Ritz in his PhD thesis (James, 2006). Tita, V., et al. reported experimental and numerical approaches in their paper (Tita, 2008), however the numerical approach uses fracture mechanics for failure mechanism and prediction.

Literature search led that since the middle of 1980's the damage characteristics similar to that induced during quasi-static tests under the transverse loads had been studied experimentally. Significant efforts were directed toward developing numerical methods but the phenomena were only started to be modelled during the 1990's. A few experimental studies have measured the residual velocity of various laminates under a range of striking velocities.

Modelling focused on determining the impact load for initializing damage and relationship between the load and damage area were studied using Hashin's failure criterion to predict matrix cracks with empirical relations of in-plane shear. A model for Kevlar-29-polyester laminates penetrated by a conical faced projectile which used a finite-difference scheme to capture the assumed local and

global deformation modes. The model based on the static punch curve to characterize the damage process was used to predict the energy needed to completely fail the specimen in 1993.

The above studies, empirical relations and the semi-analytical models are proposed to attack these geometric and material nonlinear problems. Solutions of the existing analytical techniques provide some understanding and predictive capabilities for application in preliminary damage resistance. However, composites are complex in nature and many of their characteristics still remain mysterious. Analysis of such problems and enhanced performance of composites for damage resistance cannot be fully utilised through the experimental and analytical methods.

Thus, the previous works focus on developing the phenomenological models and the semi-analytical models by making appropriate assumptions based on the experimental observation. Therefore, a suitable computational model is essential to exploit the full benefits of the advanced composites. Hence, the problem was transformed into numerical predictions to obtain adequate, consistent and reliable results.

2. Mathematical Formulations

Inherent modelling complications with impact damage simulation occur when a lamina is damaged, as properties of the laminate change according to stiffness degradation. This generates the complex iterative process of obtaining nonlinear equilibrium equations and their solutions each time a local material sub-model changes and continues until no additional lamina damage/failure are detected. Such damage introductions were considered by reduction of elastic constants from stiffness matrices.

The proposed methodology is based on the concept that the low velocity impact response is similar to the deformation due to static transverse load. A laminated composite panel of length ‘a’, breadth ‘b’ and ‘h’ with n arbitrary oriented layers is considered. The dimension ‘a’ is large as compared to ‘b’ and very large to the other ‘h’. To study the impact event as a static global bending, by neglecting the inertia forces the problem reduces to a static equivalent one. The behaviour of an elastic material under load is governed by its stress-strain characteristics known as Hook’s Law. In the present case a lamina in plane stress and let the 1-2 axes shown in Figure 1 be aligned with the fibre axis. In plane stress we assume the lamina is very thin and the stress through the lamina thickness is very small.

Figure 1: Lamina axes defined as local (1, 2) and global (x, y)

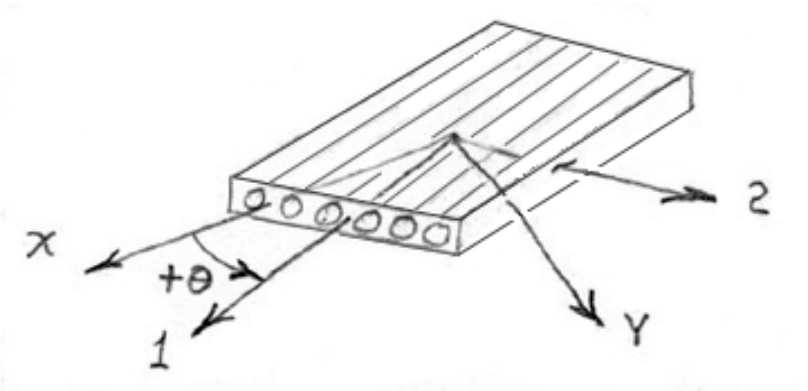

$$\begin{Bmatrix} \sigma_1 \\ \sigma_2 \\ \tau_{12} \end{Bmatrix} = \begin{bmatrix} Q_{11} & Q_{12} & 0 \\ Q_{12} & Q_{22} & 0 \\ 0 & 0 & 2Q_{66} \end{bmatrix} \begin{Bmatrix} \varepsilon_1 \\ \varepsilon_2 \\ \gamma_{12}/2 \end{Bmatrix} \quad (2\text{-}1)$$

The elements of [Q] are related to the engineering constants E,G, and ν as follows

$$Q_{11} = \frac{E_{11}}{1 - \nu_{12}\nu_{21}}, \; Q_{22} = \frac{E_{22}}{1 - \nu_{12}\nu_{21}}, \; Q_{12} = \frac{\nu_{21} E_{11}}{1 - \nu_{12}\nu_{21}} = \frac{\nu_{12} E_{22}}{1 - \nu_{12}\nu_{21}}, \tag{2-2}$$

$$Q_{66} = G_{12} \quad \text{and} \quad \nu_{21} E_{11} = \nu_{12} E_{22} \tag{2-3}$$

Transformation of lamina stress and strain from the 1-2 axes to the rotated x-y axes is shown here in matrix notation.

$$\{\sigma\} = [T]\{\sigma\}_x$$
$$\{\varepsilon\} = [T]\{\varepsilon\}_x \tag{2-4}$$

where

$$[T] = \begin{bmatrix} \cos^2\theta & \sin^2\theta & 2\sin\theta\cos\theta \\ \sin^2\theta & \cos^2\theta & -2\sin\theta\cos\theta \\ -\sin\theta\cos\theta & \sin\theta\cos\theta & (\cos^2\theta - \sin^2\theta) \end{bmatrix} \tag{2-5}$$

The lamina stress-strain relationship in the rotated x-y coordinates

$$\begin{Bmatrix} \sigma_x \\ \sigma_y \\ \tau_{xy} \end{Bmatrix} = \begin{bmatrix} \bar{Q}_{11} & \bar{Q}_{12} & 2\bar{Q}_{16} \\ \bar{Q}_{12} & \bar{Q}_{22} & 2\bar{Q}_{26} \\ \bar{Q}_{16} & \bar{Q}_{26} & 2\bar{Q}_{66} \end{bmatrix} \begin{Bmatrix} \varepsilon_x \\ \varepsilon_y \\ \gamma_{xy}/2 \end{Bmatrix} \tag{2-6}$$

Deflections are assumed small and the Kirchoff thin plate approximations can be used here to derive relationships between in-plane and out-of-plane displacements, curvatures, twists, in-plane u_o and v_o displacements are augmented by out-of-plane (Z-direction) displacements and rotations.

$$u = u_o - z\frac{\partial w}{\partial x}, \; v = v_o - z\frac{\partial w}{\partial y} \tag{2-7}$$

The strain-displacement relationships are rewritten here for components of displacement, u and v, confined to the x-y plane ("in-plane").

$$\varepsilon_x = \frac{\partial u}{\partial x}, \; \varepsilon_y = \frac{\partial v}{\partial y}, \; \gamma_{xy} = \frac{\partial u}{\partial y} + \frac{\partial v}{\partial x} \tag{2-8}$$

From the expression of radius of curvature, ρ, we derive expressions for curvature, k_x and k_y assuming small angular deflections.

$$k_x = 1/\rho = -\frac{\partial^2 w}{\partial x^2} \Big/ \left[1 - \left(\frac{\partial w}{\partial x}\right)^2\right]^{\frac{3}{2}}, \quad \frac{\partial w}{\partial x} \ll 1, \; k_x = -\frac{\partial^2 w}{\partial x^2}$$
$$\text{similarly } k_y = -\frac{\partial^2 w}{\partial y^2} \tag{2-9}$$

$$k_{xy} = -2\frac{\partial^2 w}{\partial x \partial y} \tag{2-10}$$

Combining equations (2-10) and (2-9), into (2-8) yields

$$\begin{Bmatrix} \varepsilon_x \\ \varepsilon_y \\ \gamma_{xy} \end{Bmatrix} = \begin{Bmatrix} \varepsilon_x^o \\ \varepsilon_y^o \\ \gamma_{xy}^o \end{Bmatrix} + \begin{Bmatrix} k_x \\ k_y \\ k_{xy} \end{Bmatrix} \tag{2-11}$$

Substituting equation (2-11) into equation (2-6) yields a more general stress-strain relationship for the k-th lamina which includes out-of-plane displacement implicitly in the curvature terms.

$$\begin{Bmatrix} \sigma_x \\ \sigma_y \\ \tau_{xy} \end{Bmatrix} = \begin{bmatrix} \bar{Q}_{11} & \bar{Q}_{12} & \bar{Q}_{16} \\ \bar{Q}_{12} & \bar{Q}_{22} & \bar{Q}_{26} \\ \bar{Q}_{16} & \bar{Q}_{26} & \bar{Q}_{66} \end{bmatrix}_k \left\{ \begin{Bmatrix} \varepsilon_x^o \\ \varepsilon_y^o \\ \gamma_{xy}^o \end{Bmatrix} + Z_k \begin{Bmatrix} k_x \\ k_y \\ k_{xy} \end{Bmatrix} \right\} \tag{2-12}$$

With stresses defined in terms of the Z-coordinate, through the laminate thickness, integrating these expressions to get the laminate resultant in-plane loads (N_x, N_y, N_{xy}), and moments (M_x, M_y, M_{xy}).

Figure 2: in-plane loads and moments

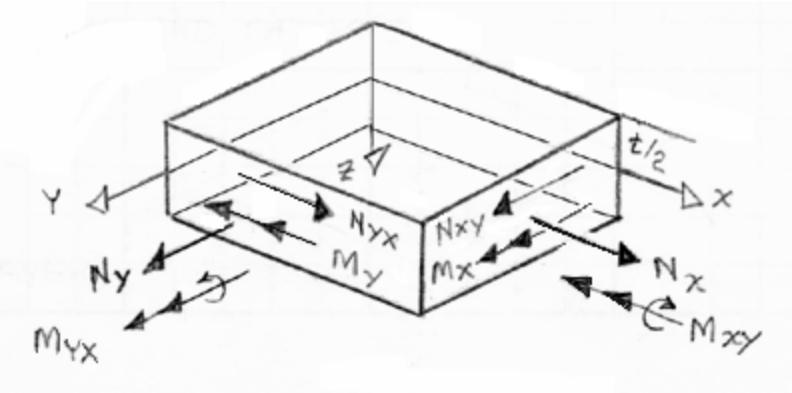

$$\begin{Bmatrix} N_x \\ N_y \\ N_{xy} \end{Bmatrix} = \int_{-\frac{t}{2}}^{\frac{t}{2}} \begin{Bmatrix} \sigma_x \\ \sigma_y \\ \tau_{xy} \end{Bmatrix} dz = \sum_{k=1}^{n} \int_{-Z_{k-1}}^{Z_k} \begin{Bmatrix} \sigma_x \\ \sigma_y \\ \tau_{xy} \end{Bmatrix}_k dz \,, \quad \begin{Bmatrix} M_x \\ M_y \\ M_{xy} \end{Bmatrix} = \int_{-\frac{t}{2}}^{\frac{t}{2}} \begin{Bmatrix} \sigma_x \\ \sigma_y \\ \tau_{xy} \end{Bmatrix} z dz = \sum_{k=1}^{n} \int_{-Z_{k-1}}^{Z_k} \begin{Bmatrix} \sigma_x \\ \sigma_y \\ \tau_{xy} \end{Bmatrix}_k z dz \tag{2-13}$$

Substitute equation (2-12) into equation (2-13) and simplify.

$$\begin{Bmatrix} N_x \\ N_y \\ N_{xy} \end{Bmatrix} = \sum_{k=1}^{n} \left\{ \begin{bmatrix} \bar{Q}_{11} & \bar{Q}_{12} & \bar{Q}_{16} \\ \bar{Q}_{12} & \bar{Q}_{22} & \bar{Q}_{26} \\ \bar{Q}_{16} & \bar{Q}_{26} & 2\bar{Q}_{66} \end{bmatrix}_k \begin{Bmatrix} \varepsilon_x^o \\ \varepsilon_y^o \\ \gamma_{xy}^o \end{Bmatrix} \int_{-Z_{k-1}}^{Z_k} dz + \begin{bmatrix} \bar{Q}_{11} & \bar{Q}_{12} & \bar{Q}_{16} \\ \bar{Q}_{12} & \bar{Q}_{22} & \bar{Q}_{26} \\ \bar{Q}_{16} & \bar{Q}_{26} & 2\bar{Q}_{66} \end{bmatrix}_k \begin{Bmatrix} k_x \\ k_y \\ k_{xy} \end{Bmatrix} \int_{-Z_{k-1}}^{Z_k} z dz \right\},$$

$$\begin{Bmatrix} M_x \\ M_y \\ M_{xy} \end{Bmatrix} = \sum_{k=1}^{n} \left\{ \begin{bmatrix} \bar{Q}_{11} & \bar{Q}_{12} & \bar{Q}_{16} \\ \bar{Q}_{12} & \bar{Q}_{22} & \bar{Q}_{26} \\ \bar{Q}_{16} & \bar{Q}_{26} & 2\bar{Q}_{66} \end{bmatrix}_k \begin{Bmatrix} \varepsilon_x^o \\ \varepsilon_y^o \\ \gamma_{xy}^o \end{Bmatrix} \int_{-Z_{k-1}}^{Z_k} z dz + \begin{bmatrix} \bar{Q}_{11} & \bar{Q}_{12} & \bar{Q}_{16} \\ \bar{Q}_{12} & \bar{Q}_{22} & \bar{Q}_{26} \\ \bar{Q}_{16} & \bar{Q}_{26} & 2\bar{Q}_{66} \end{bmatrix}_k \begin{Bmatrix} k_x \\ k_y \\ k_{xy} \end{Bmatrix} \int_{-Z_{k-1}}^{Z_k} z^2 dz \right\} \tag{2-14}$$

Equation (2-14) can be simplified where

$$A_{ij} = \sum_{k=1}^{n} \left(\bar{Q}_{ij}\right)_k \left(z_k - z_{k-1}\right), \; B_{ij} = \frac{1}{2} \sum_{k=1}^{n} \left(\bar{Q}_{ij}\right)_k \left(z_k^2 - z_{k-1}^2\right), \; D_{ij} = \frac{1}{3} \sum_{k=1}^{n} \left(\bar{Q}_{ij}\right)_k \left(z_k^3 - z_{k-1}^3\right) \tag{2-15}$$

The relative position of each k-th lamina used by equation (2-13) to integrate through the thickness to calculate the laminate loads, (N_x, N_y, N_{xy}), and moments (M_x, M_y, M_{xy}).

Figure 3: Laminate configuration for integration of through the thickness plies

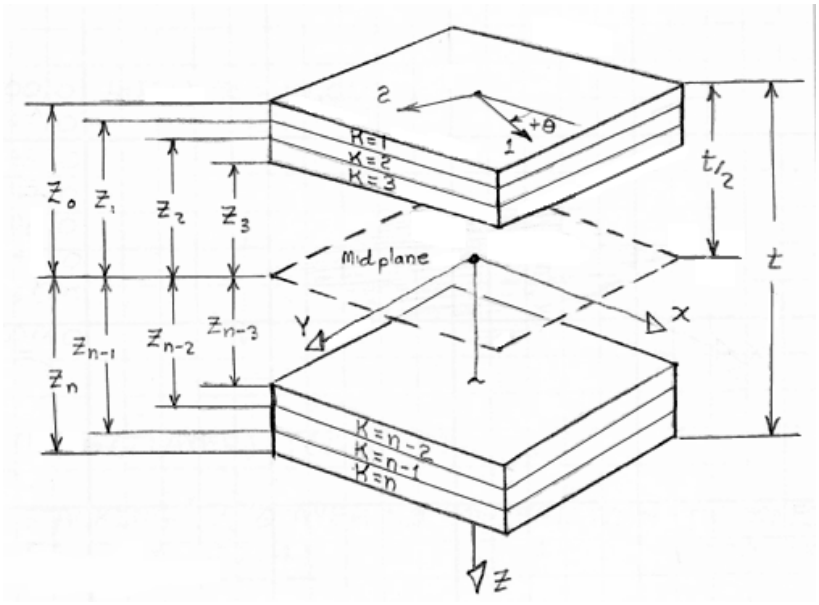

For the case of a thin, orthotropic laminate in a state of plane stress, the differential equation of static equilibrium is:

$$D_{11}\frac{\partial^4 w}{\partial x^4} + 2\left(D_{12} + 2D_{66}\right)\frac{\partial^4 w}{\partial x^2 \partial y^2} + D_{22}\frac{\partial^4 w}{\partial y^4} = q(x,y) \tag{2-16}$$

Where the external load could be point, line or uniformly distributed external load.

When an impact event occurs to a composite panel, visible damage is not always apparent although there can be severe underlying damage. Static indentation and quasi-static indentation techniques are used in which a specimen can be loaded in increment of force over an infinite period of time. A correlation between the measurable dent-depth (visible damage) is made to address the damage resistance. This aspect was considered and also modified as static load-deflection with pseudo-damage. Analysis was also carried out to find out the deflections due to virgin and induced pseudo-damage models.

The standard procedure to simulate an impact event is using a static or quasi-static loading which has been proved to be very useful. Using this procedure, damage initiation and progression can be more easily detected as deflection can be directly measured with great accuracy, and maximum transverse force can be better controlled. Simulation for load-deflection was also carried out for virgin and pseudo-damage models.

3. Strength and Failure Theories

Various theories based on the normal and shear strengths of lamina have been developed. The stresses acting on the lamina are resolved into the normal and shear stresses in the local axes. In case of a unidirectional lamina, there are two material axes, one which is parallel to the fibres and one which is perpendicular to the fibres. Hence, there are four normal strength parameters for a unidirectional lamina, one for tension and one for compression, in each of the two material axes directions. The fifth strength parameter is the shear strength of a unidirectional lamina. The shear stress, whether positive or negative, does not have an effect on the reported shear strengths of a unidirectional lamina.

Unlike the stiffness parameters, these strength parameters cannot be transformed directly for an angle lamina. Hence, the failure theories are based on first finding the stresses in the local axes and then using these five strength parameters to find whether a lamina has failed. Failure is predicted in a

lamina, if any of the normal or shear stresses in the local axes are equal or exceed the corresponding ultimate strengths. Given the stresses or strains in the global axes stresses in the material axes can be found.

3.1. Tsai-Hill Failure Theory

This theory is based on distortion energy failure theory of Von-Mises distortional energy yield criterion for isotropic materials as applied to anisotropic materials. Distortion energy in a body consists of two parts –one due to a change in volume and is called the dilation energy and the second due to a change in shape and is called the distortion energy. It is assumed that failure takes place only when the distortion energy is the greater than the failure distortion energy. It was Hill who adopted the Von. Mises distortional energy yield criterion to anisotropic materials. Then Tsai adapted it to a unidirectional lamina. Based on the theory, Tsai proposed that a lamina has failed if

$$(G_2+ G_3)\ \sigma_1^2 + (G_1+ G_3)\ \sigma_2^2 + (G_1 + G_2)\ \sigma_3^2 - 2G_3\ \sigma_1\ \sigma_2 - 2G_2\ \sigma_1\ \sigma_3 - 2G_1\ \sigma_2\ \sigma_3 + 2G_4\ \tau_{23}^2 + 2G_5\ \tau_{13}^2 + 2G_6\ \tau_{12}^2 < 1 \quad (3\text{-}1)$$

is violated. The components G_1, G_2, G_3, G_4, G_5, G_6, of the strength criterion depend on the failure strengths and are found as follows.

1. Applying $\sigma_1 = \left(\sigma_1^T\right)_{ult}$ to a unidirectional lamina, then the lamina will fail. Hence above equation reduces to
   $$(G_2+ G_3)\ \left(\sigma_1^T\right)_{ult}^2 = 1 \quad (3\text{-}2)$$
2. Applying $\sigma_2 = \left(\sigma_2^T\right)_{ult}$ to a unidirectional lamina, then the lamina fail and equation reduces to
   $$(G_1 + G_2)\ \left(\sigma_2^T\right)_{ult}^2 = 1 \quad (3\text{-}3)$$
3. Applying $\sigma_3 = \left(\sigma_2^T\right)_{ult}$ to a unidirectional lamina, and assuming that the normal tensile failure strength is the same in direction (3-2) and (3-3), the lamina will fail. hence the equation reduces to
   $$2G_6\ \left(\tau_{12}\right)_{ult}^2 = 1 \quad (3\text{-}4)$$
   From equation -- ,
   $$G_1 = \frac{1}{2}\left[\frac{2}{\left[\left(\sigma_2^T\right)_{ult}^2\right]^2} - \frac{1}{\left[\left(\sigma_1^T\right)_{ult}^2\right]^2}\right] \quad (3\text{-}5)$$
   $$G_2 = \frac{1}{2}\left[\frac{2}{\left[\left(\sigma_1^T\right)_{ult}\right]^2}\right] \quad (3\text{-}6)$$
   $$G_3 = \frac{1}{2}\left[\frac{2}{\left[\left(\sigma_1^T\right)_{ult}\right]^2}\right] \quad (3\text{-}7)$$
   $$G_6 = \frac{1}{2}\left[\frac{2}{\left[\left(\tau_{12}\right)_{ult}\right]^2}\right] \quad (3\text{-}8)$$

Since the unidirectional lamina is assumed to be under plane stress, that is, $\sigma_3 = \tau_{31} = \tau_{23} = 0$, the equation reduces to

$$\left[\frac{\sigma_1}{\left(\sigma_1^T\right)_{ult}}\right]^2 - \left[\frac{\sigma_1\sigma_2}{\left(\sigma_1^T\right)_{ult}^2}\right] + \left[\frac{\sigma_2}{\left(\sigma_2^T\right)_{ult}}\right]^2 + \left[\frac{\tau_{12}}{\left(\tau_{12}\right)_{ult}}\right]^2 < 1 \quad (3\text{-}9)$$

Given the global stresses the local stresses can be found apply the above theory to determine whether or not the lamina has failed.

3.2. Tsai-Wu Failure Theory

This failure theory is based on the total strain energy failure theory of Beltami. Tsai and Wu applied failure theory to a lamina in plane stress. A lamina is considered to be failed if

$$H_1 \sigma_1 + H_2 \sigma_2 + H_6\tau_{12} + H_{11}\sigma_1^2 + H_{22}\sigma_2^2 + H_{66}\tau_{12}^2 + H_{12}\sigma_2\sigma_1 < 1 \quad (3\text{-}10)$$

is violated. This theory is more general than the Tsai-Hill failure theory as it distinguishes between the compressive and tensile strengths of a lamina. The components H_1, H_2, H_6, H_{11}, H_{22}, H_{66}, of the theory are found using the five strength parameters of a unidirectional lamina as follows.

1. Applying $\sigma_1 = \left(\sigma_1^T\right)_{ult}$, $\sigma_2 = 0$, $= \tau_{12} = 0$ to a unidirectional lamina, then the lamina will fail. Hence above equation reduces to
   $$H_1 \left(\sigma_1^T\right)_{ult} + H_{11}\left(\sigma_1^T\right)^2_{ult} = 1 \quad (3\text{-}11)$$
2. Applying $\sigma_1 = -\left(\sigma_1^C\right)_{ult}$, $\sigma_2 = 0$, $= \tau_{12} = 0$ to a unidirectional lamina, then the lamina fail and equation reduces to
   $$-H_1 \left(\sigma_1^C\right)_{ult} + H_{11}\left(\sigma_1^C\right)^2_{ult} = 1 \quad (3\text{-}26)$$
   From Equations (3-) and (3-),
   $$H_1 = \frac{1}{\left(\sigma_1^T\right)_{ult}} - \frac{1}{\left(\sigma_1^C\right)_{ult}} \quad (3\text{-}12)$$
   $$H_{11} = \frac{1}{\left(\sigma_1^T\right)_{ult}} \frac{1}{\left(\sigma_1^C\right)_{ult}} \quad (3\text{-}13)$$
3. Applying $\sigma_1 = 0$, $\sigma_2 = \left(\sigma_2^T\right)_{ult}$, $= \tau_{12} = 0$ to a unidirectional lamina, then the lamina fail and equation reduces to
   $$H_2 \left(\sigma_2^C\right)_{ult} + H_{22}\left(\sigma_2^C\right)^2_{ult} = 1 \quad (3\text{-}14)$$
4. Applying $\sigma_1 = 0$, $\sigma_2 = -\left(\sigma_2^C\right)_{ult}$, 0, $= \tau_{12} = 0$ to a unidirectional lamina, then the lamina fail and equation reduces to
   $$-H_2 \left(\sigma_2^C\right)_{ult} + H_{22}\left(\sigma_2^C\right)^2_{ult} = 1 \quad (3\text{-}15)$$
   $$H_2 = \frac{1}{\left(\sigma_2^T\right)_{ult}} - \frac{1}{\left(\sigma_2^C\right)_{ult}} \quad (3\text{-}16)$$
   $$H_{22} = \frac{1}{\left(\sigma_2^T\right)_{ult}} \frac{1}{\left(\sigma_{21}^C\right)_{ult}} \quad (3\text{-}17)$$
5. Applying $\sigma_1 = 0$, $\sigma_2 = 0$, $= \tau_{12} = \left(\tau_{12}\right)_{ult}$ to a unidirectional lamina, then the lamina fail and equation reduces to
   $$H_6 \left(\tau_{12}\right)_{ult} + H_{66}\left(\tau_{12}\right)^2_{ult} = 1 \quad (3\text{-}18)$$
6. Applying $\sigma_1 = 0$, $\sigma_2 = 0$, $= \tau_{12} = -\left(\tau_{12}\right)_{ult}$ to a unidirectional lamina, then the lamina fail and equation reduces to
   $$-H_6\left(\tau_{12}\right)_{ult} + H_{66}\left(\tau_{12}\right)^2_{ult} = 1 \quad (3\text{-}19)$$
   From Equations (3-5) and (3-6)
   $$H_6 = 0, \quad (3\text{-}20)$$
   $$H_{66} = \frac{1}{\left(\tau_{12}\right)^2_{ult}} \quad (3\text{-}21)$$

The only component of the theory which cannot be found directly from the five strength parameters of the unidirectional lamina is H_{12}. This can be found experimentally by knowing a biaxial stress at which the lamina fails and then substituting values of σ_1, σ_2, and τ_{12}. Note that σ_1 and σ_2 both need to be nonzero to find H_{12}. Experimental methods to find H_{12} include the following.

1. Applying equal tensile loads along the two material axes in a unidirectional composite. If $\sigma_x = 0$, $\sigma_y = 0$, $= \tau_{xy} = 0$ is the load at which the lamina fails, then
   $(H_1 + H_2)\,\sigma + (H_{11} + H_{22} + H_{12})\,\sigma^2 = 1$ (3-22)
   The solution of Equation gives
   $H_{12} = 1/\sigma^2\,[1 - H_1 + H_2)\sigma + (H_{11} + H_{22})\,\sigma^2$ (3-23)
   It is necessary to pick tensile loads in the above biaxial test, but one may apply any combination of
   $\sigma_1 = \sigma, \sigma_2 = 0;\ \sigma_1 = -\sigma, \sigma_2 = -\sigma;\ \sigma_1 = -\sigma, \sigma_2 = \sigma$ (3-24)
   This will give four displacement values of H_{12}, each corresponding to the four tests.
2. Take a 45º lamina under uniaxial tension σ_x. This stress σ_x at failure is noted. If this stress is $\sigma_x = \sigma$, then using the local stresses at failure are
   $\sigma_1 = \sigma/2;\ \sigma_2 = \sigma/_2;\ \tau_{12} = -\sigma/2$ (3-25)
   Substituting the above local stresses in Equation (3-11),
   $(H_1 + H_2)\,\sigma/2 + \sigma^2/4[H_{11} + H_{22} + H_{66} + 2H_{12}) = 1$ (3-28)
   $H_{12} = 2/\sigma^2 - (H_1 + H_2)/\sigma - (H_{11} + H_{22} + H_{66})$ (3-27)
   There are also some empirical suggestions for finding the value of H_{12} which include
   $H_{12} = -\frac{1}{2\left(\sigma_1^T\right)_{ult}^2}$ as per Tsai-Hill failure theory (3-28)
   $H_{12} = -\frac{1}{2\left(\sigma_1^T\right)_{ult}\left(\sigma_1^C\right)_{ult}}$ as per Hoffman criteria (3-29)
   $H_{12} = -\frac{1}{2}\sqrt{\frac{1}{\left(\sigma_1^T\right)_{ult}\left(\sigma_1^C\right)_{ult}\left(\sigma_2^T\right)_{ult}\left(\sigma_2^C\right)_{ult}}}$ as per Mises_Hencky criterion (3-30)

The stresses in an individual lamina are fundamental to control the failure initiation and progression in the laminate. The strength of each lamina was assessed separately by considering the stresses acting on it along material axes. The initial failure of a lamina (first ply failure) was governed by exceeding the maximum limit prescribed by failure criteria. The determination of the first ply failure load was very essential in understanding the failure process as well as the reliability of structures. Tsai-Wu quadratic failure criterion is chosen for predicting the initiation of matrix cracking.

4. Development of Computational Model

Finite Element Method (FEM) has received a tremendous attention in engineering and industry because of its diversity and flexibility as an analysis tool. Solutions to physical problems can be obtained very effectively and to a high degree of accuracy using FEM software packages program for a number of problems including this type of work.

Since modelling of the location of the critical damage region under impactors is a very complicated phenomenon because of the damage accumulates into through-the-thickness of the specimen and internal loads re-distribution after impact. Hence, transformation of mathematical formulations into FEM numerical model and writing modular code need extensive efforts and time. There is an efficient way to solve the problems using software generated simulation. For this work, commercially available software ABAQUS, which incorporates shell elements and simulation stacks of shell elements, was selected. The user table option in ABAQUS provides an extended amount of input data without having to re-link the code that could be utilised for various trials.

A laminated composite laminate of diameter 23.94 mm, with 2.88 mm thickness of quasi-isotropic configuration under centrally located load of 70 MPa at circle of 6.3 mm diameter was studied for various data input and stacking sequences and clamped boundary conditions. The properties of a unidirectional lamina of specimens with geometries in Fig 4 below and data are given in the following Table 1, and damaged ply properties are given in Table 2:

Figure 4: Fully clamped Model under Out-of-Plane Central Load

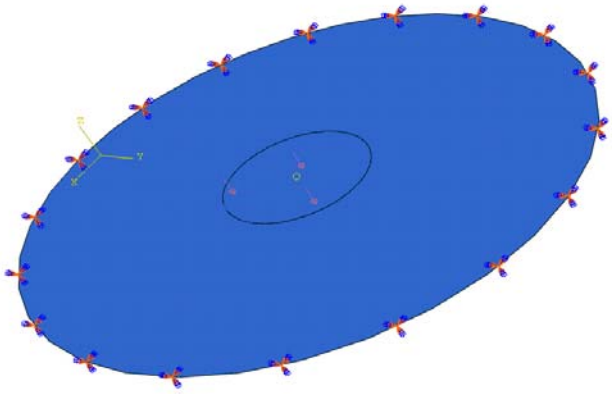

Table 1: Input Data

Material Properties	Ultimate Strengths	Stacking Sequences
E_1 = 150 GPa, $E_2 = E_3$ = 15 GPa	$(\sigma^{T}_{1})_{ult}$ = 1500 MPa	$[45/0/-45/90]_{S,}$ $[45/0/-45/90]_{2S,}$ $[45/0/-45/90]3_S$
	$(\sigma^{C}_{1})_{ult}$ = 1500 MPa	
G_{12} = 5.7 GPa G_{13} = 5.7 Gpa G23 =7.26 GPa	$(\sigma^{T}_{2})_{ult}$ = 40 MPa	
Poisson's Ratios ν_{12} = 0.33 ν_{23} = 0.03 ν_{13} = 0.01	$(\sigma^{C}_{2})_{ult}$ = 20 MPa	
	$(\tau_{12})_{ult}$ = 53 MPa	

Table 2: Input Data

Material Properties	Ultimate Strengths	Stacking Sequences
E_1 = 2 GPa, $E_2 = E_3$ = 1 GPa	$(\sigma^{T}_{1})_{ult}$ = 1500 MPa $(\sigma^{C}_{1})_{ult}$ = 1500 MPa	$[45/0/-45/90]_{S,}$ $[45/0/-45/90]_{2S,}$ $[45/0/-45/90]3_S$
G_{12} = 0.5 GPa G_{13} = 0.5 Gpa G23 = 0.5	$(\sigma^{T}_{2})_{ult}$ = = 40 MPa	
Poisson's Ratios ν_{12} = 0.33 ν_{23} = 0.03 ν_{13} = 0.01	$(\sigma^{C}_{2})_{ult}$ = 20 MPa	
	$(\tau_{12})_{ult}$ = 53 MPa	

Damage was induced as areas of these weaker material properties Table 2 under the load areas in ply-by-ply fashion until failure was achieved.

5. Numerical Results and Discussion

Simulations were carried out for three sets of symmetric stacking sequences for plies 8, 16, and 24. Models were run to obtain stresses as well as displacements for virgin, pseudo-damaged ply and progressive induction of pseudo-damaged plies to record the numerical results. Obtained values for stresses were used and compared against their strength values in Tsai-Hill and Tsai-Wu criteria to

predict failure for undamaged, damaged, and damaged up to failure. Selected results from the first four plies of the 24-ply model $[45/0/-45/90]3_S$ were presented here as bulk of the output was too much.

Figure 5: Output Legend Table and Stresses (σ_{11}) Contour Plots from Un-Damaged Model

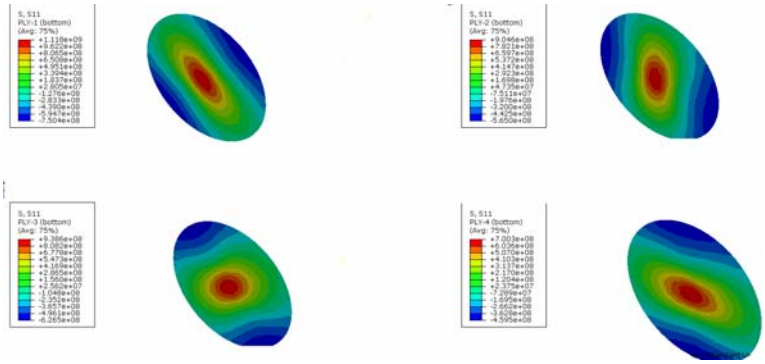

Looking at the input data table for strength values and un-damaged stresses in principal directions in this data table and contours and comparing them with the given strength values it could be seen that no ply was failed.

Figure 6: Un-Damaged Model's Output Legend Table and Contours Plots of Stresses (σ_{22})

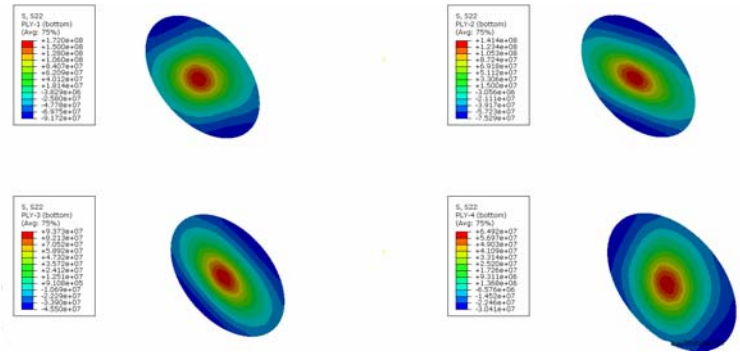

Looking at the input data table for strength values and un-damaged stresses in transverse directions in this data table and contours and comparing them it could be seen that no ply was failed.

Figure 7: Output Legend Tables and Contour Plots of Stresses (τ_{12}) from Un-Damaged Model

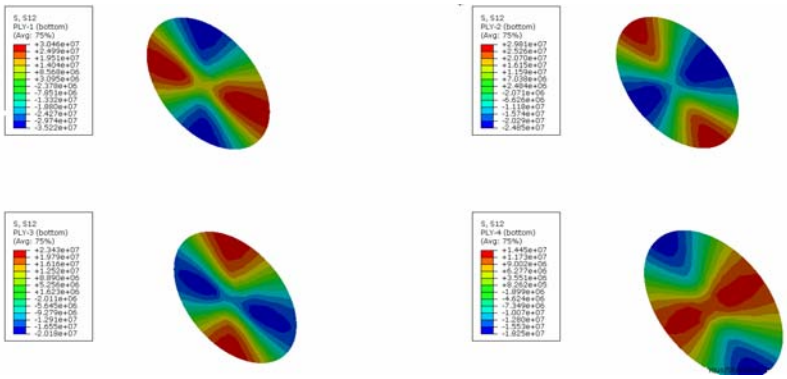

Looking at the input data table for strength values and un-damaged stresses in in-plane shear stresses in this data table and contours and comparing them it could be seen that no ply was failed. Using the given strength parameters and the computed stresses in the Tsai-Hill and Tsai-Wu criteria it was found that no ply fails.

Figure 8: Output Legend Tables and Displacements Contours from Un-Damaged Model

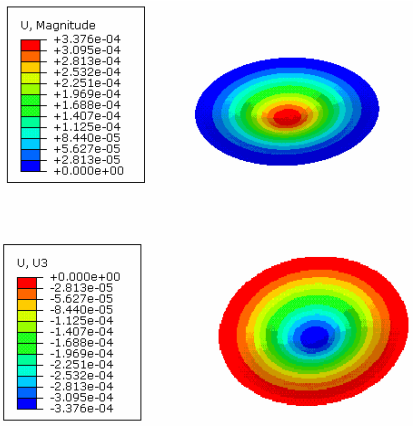

Magnitude and displacement values in the out-of-plane direction shown that there was no abrupt change in the values and values were reasonable means that no ply fails under the applied load (constant load).

Figure 9: Output Legend Tables and Contour Plots of Plies 11 and 12 Damaged (σ_{11}): First Ply Fails

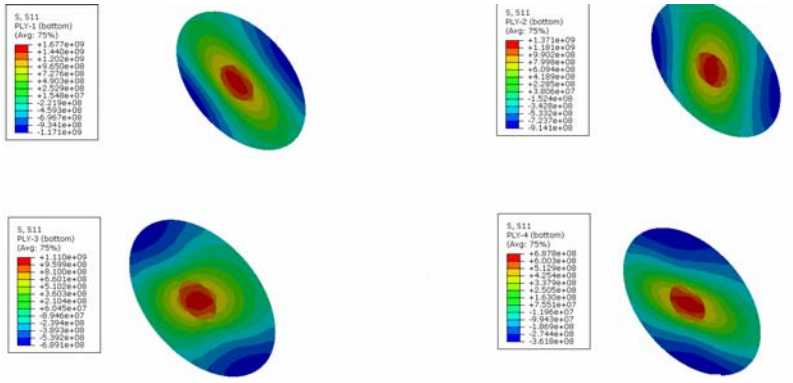

Looking at the input data table for strength values and computed stresses from damaged model in principal directions in this data table and contours and comparing them it could be seen that a ply was failed.

Figure 10: Output Legend Tables and Contour Plots of Plies 11 & 12 Damaged (σ_{22}) when First Ply Fails

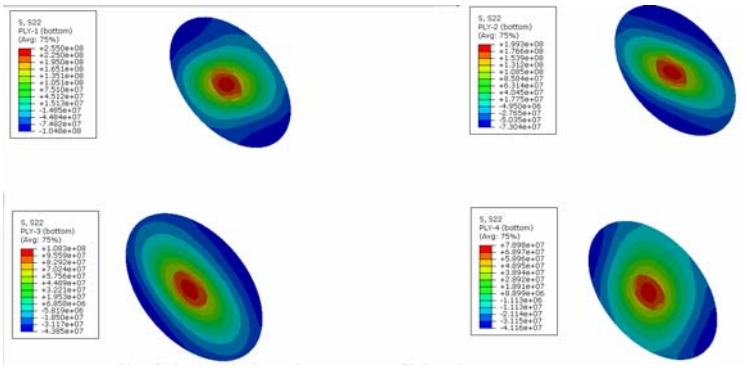

Looking at the input data table for strength values and computed stresses from damaged model in transverse direction in this data table and contours and comparing them it could be seen that a ply was failed.

Figure 11: Output Legend Tables and Contour Plots of Plies 11 & 12 Damaged (τ_{12}) when First Ply Fails

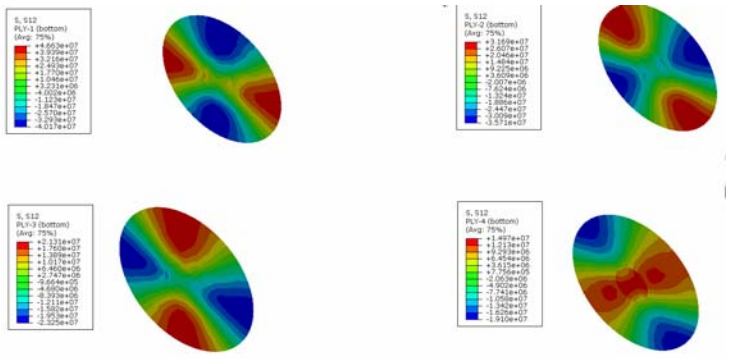

Looking at the input data table for strength values and computed stresses from damaged model in in-plane stresses in this data table and contours and comparing them it could be seen that a ply was failed. Using the given strength parameters and the computed stresses in the Tsai-Hill and Tsai-Wu criteria it was found that a ply fails.

Figure 12: Output legend Table and Displacement Contours from Damaged Model

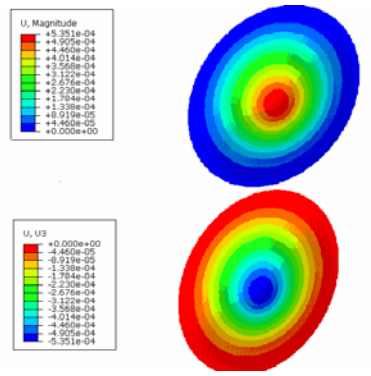

Magnitude and displacement values in the out-of-plane direction shown that there was a change in the values and values were bigger than the un-damaged model means that a ply was failed under the applied load (constant load).

The computational model for load-deflection generates the numerical results to study the transverse bending to correlate it with stiffness degradations. The deflection considered in each lamina was the same for each case.

To further improve the convergence and results' validity, adaptive meshing techniques were applied to obtain fine meshes for high stress regions (area under load) and coarse meshes for the rest. Output results, table and graphs for all the sets were too much so a few of them were selected and included here.

6. Conclusion

The project successfully modelled the impact damage as a damage-induced impact. The estimates were found in good agreement with the available literature.

The analysis presented found to be simple to predict the extent of damage and failure using the standard criteria, which provides opportunity to effectively describe the progressive damaged

behaviour of composite panels. The work shows that one of the governing factors in the impact damage resistance is the pseudo-damage. Performance of the laminates could be properly tailored by controlling the strength parameters for the design against failure. The availability of such a code will greatly facilitate the development of composite panels with enhanced impact resistance capacity.

References

[1] Elber, W., Effect of matrix and fibre properties on impact resistance, *Tough Composite Materials: Recent developments,* Noyes, Park Ridge, NJ, 1985, pp. 89-110.

[2] Sierakowski, R. L., and Chaturvedi, S. C., Dynamic Loading and Characterization of Fibre-Reinforced Composites, John Wiley & Sons, Inc.,1997.

[3] Matsumoto, H., Ogwa, Y. and Adchi, T., Stress analysis of an orthotropic laminated slab to transverse load, *JSME Series*, I, Vol.35(2), 1992, pp.165-169.

[4] Choi, H.Y., Downs, R. J., and Chang, F. K., A new approach to damage mechanisms and mechanics of composites due to low-velocity impact: Part I- experiments, Part II- Analysis, *Journal of Composite Materials*, Vol.25, (1991), pp. 992-1038.

[5] Choi, H.Y. and Chang, F. K., A predicting model for graphite/epoxy composites low-velocity impact, *Journal of Composite Materials*, Vol. 26, No. 14, (1992), pp. 2134-2169.

[6] Sun, C. T. and Jih, C. J., A quasi-static treatment of de-lamination crack in laminates subjected to low velocity impact, Proceedings of 7th Technical Conference of ASC, Pennsylvania State University, October 13-15, pp. 949-961.

[7] Zhu, G., Goldsmith, W., and Dharan, C. K. H., Penetration of kevlar by projectiles- I. Exp investigation, *International Journal of Solids and Structures*, Vol. 29 (1992), pp. 421-436.

[8] Wu, E., Tsai, C. Z. and Chen, Y. C., Penetration of glass/epoxy composite laminates, *Journal of Composite Materials*, Vol.28, (1994), pp. 1783-1802.

[9] Abrate, S., Impact on laminated composites: recent advances, *Applied Mechanics Reviews*, Vol. 47, No. 11 (1994), pp.517-544.

[10] Goldsmith, W., Dharan, C. K. H., and Chang, H., Quasi-static ballistic perforation of carbon fibre laminates, *Int Journal of Solids and Struct,* Vol. 32, No.1 (1995), pp. 89-103.

[11] Sun, C. T. and Potti, S. V., A model to predict residual velocity of thick composite to high velocity impact, *Int Journal of Impact Engineering*, Vol.18, No.3 (1996), pp. 339-353.

[12] Lee, S. W. R. and Sun, C. T., A quasi-static penetration model for composite laminates, *Journal of Composite Materials*, Vol.27 (1993), pp. 251-271.

[13] Greif, R. and Chapon, E, Investigation of successive failure modes in graphite epoxy comp panels, *Journal of Reinforced Plastics and Composites*, Vol. 12 (1993), pp. 602-620.

[14] Kim, Y., Davalos, J. F. and Barbero, E. J., Progressive failure analysis of composite panels, *Journal of Composite Materials*, Vol.30, No.5 (1996), pp. 536-560.

[15] Abrate, S. Impact on laminated composite materials, Applied Mechanics Review, Vol. 44, No. 4 (1991), pp. 155-190.

[16] Luo, J.Z., Liu, T.G., Zhang, T., 2004. Three-dimensional linear analysis for composite axially symmetrical circular plate. International journal of Solid and Structures, 41: 3689-3706.

[17] James, R. A, Impact Damage Resistance and Damage Tolerance of Fibre Reinforced Laminate Composites, PhD thesis submitted at University of Bolton, UK in April 2006.

[18] ABAQUS Users' Manual, Version 6.6, ©2006 ABAQUS, Inc.

[19] Kaw, A.K., Mechanics of Composite Materials, CRC Press LLC, New York, 1997.

[20] Tita I., Carvalho, J.D., and Vanepitte, D. Failure analysis of low velocity impact on thin composite laminates: Experimental and numerical approaches, Composite and Structures, Issue 83, pp 413-428, 2008.